

Spatiotemporal Location Fingerprint Generation Using Extended Signal Propagation Model

Hee Sung Kim*, Binghao Li**, Wan Sik Choi***, Sang Kyung Sung[§]
and Hyung Keun Lee[†]

Abstract – Fingerprinting is a widely used positioning technology for received signal strength (RSS) based wireless local area network (WLAN) positioning system. Though spatial RSS variation is the key factor of the positioning technology, temporal RSS variation needs to be considered for more accuracy. To deal with the spatial and temporal RSS characteristics within a unified framework, this paper proposes an extended signal propagation mode (ESPM) and a fingerprint generation method. The proposed spatiotemporal fingerprint generation method consists of two algorithms running in parallel; Kalman filtering at several measurement-sampling locations and Kriging to generate location fingerprints at dense reference locations. The two different algorithms are connected by the extended signal propagation model which describes the spatial and temporal measurement characteristics in one frame. An experiment demonstrates that the proposed method provides an improved positioning accuracy.

Keywords: Received signal strength, Signal propagation model, Fingerprinting, Positioning

1. Introduction

As positioning technology is the key of location based services, many methods have been investigated. The received signal strength (RSS) based Wireless Local Area Network (WLAN) positioning has attracted much attention recently due to the increased deployment of WLAN access points (APs).

In the RSS based WLAN positioning methods, signal propagation models (SPMs) describing the relationship between the RSS value and the geometric distance of signal path have been extensively utilized [1-4]. According to them, it is generally known that RSS value decreases as distance increases.

It should be noted that the real RSS measurements also show time-varying characteristics. This can be easily verified if we sample and plot RSS values from a mobile device (MD) whose location is fixed. The conventional SPM cannot reflect this characteristic since it describes the signal propagation considering only the spatial geometries between the MD and the APs.

Thus, to improve the positioning accuracy, it is necessary to consider the temporal variation of RSS in addition to the geometry dependence between the MD and the APs.

The RSS based positioning technologies can be classified into two categories. One is location fingerprinting and the other is trilateration or triangulation. The former is accepted as a better method since it provides reliable location estimates in complex indoor environments.

Microsoft's RADAR [5, 6] is the first WLAN positioning system that applied fingerprinting. It was found that the fingerprint method is very time consuming and requires much labor effort. To save the labor effort and time, [7, 8], and [9], utilized the radial basis function, the Kriging algorithm and the expectation maximization algorithm, respectively. [10] proposed a method to improve accuracy by considering the precise small-scale compensation terms. [11] proposed a method to utilize extra sniffers installed at known locations for the continuous sampling of reference measurements. The sampled measurements are interpolated by applying the bi-variate interpolation algorithm [12] to generate the reference measurements on regular grid points. In [13], the inter-AP measurements are used to generate the distance mapping curves. Kaemarungsi [14] reported the experimental analysis results on RSS temporal characteristics. [15] proposed a scheme to collect reference measurements from client sniffers periodically. [16] collected reference measurements between APs. For spatial processing, a truncated singular decomposition technique was utilized to create a mapping between RSS measurements and distances. [17] introduced a comprehensive kernelized weight functions to estimate the location of an MD through the combination of the neighboring AP locations.

Based on the literature survey, it can be seen that most of previous research works focus on spatial signal

[†] Corresponding Author: School of Avionics and Telecomm., Korea Aerospace Univ. Korea (hyunlee@kau.ac.kr)

* School of Avionics and Telecomm., Korea Aerospace Univ. Korea (hskim07@kau.ac.kr)

** School of Surveying and Spatial Information Systems, UNSW, Australia (binghao.li@unsw.edu.au)

*** Electronic Research Institute, Korea (choiws@etri.re.kr)

§ Dept. Aerospace Information Eng., Konkuk Univ., Korea (sksung@konkuk.ac.kr)

characteristics. Detailed treatment of signal propagation in both spatial and temporal domains is hard to find. To deal with the spatial and temporal characteristics of the RSS within one framework, this paper proposes an efficient location fingerprint generation method based on an extended signal propagation model (ESPM).

The proposed method consists of two algorithms running in parallel; Kalman filtering at several RSS-sampling locations to compute temporal estimates and Kriging algorithm at arbitrarily many reference locations to generate the location fingerprints.

This paper is organized as follows. In Section 2, the spatiotemporal modeling is explained in the order of ESPM, temporal variation, and spatial variation. In Section 3, the Kalman filtering and Kriging algorithms are explained for location fingerprint generation. In Section 4, an experiment is introduced and the results are analyzed to demonstrate the accuracy improvement by applying the proposed method. Finally, concluding remarks are given.

2. Spatiotemporal Signal Modeling

2.1 Extended signal propagation model

To derive an efficient fingerprint generation method, a realistic signal propagation model plays a crucial role. For this purpose, an ESPM is proposed as follows.

$$\begin{aligned} \tilde{p}(s,t) &= p(s) + n(s) + m(t) + v(s,t) \\ p(s) &= p_0 - 10\alpha \log_{10} \left[\frac{d(s)}{d_0} \right] \end{aligned} \quad (1)$$

where

- $\tilde{p}(s,t)$: measured RSS (dBm)
- s : sampling location (vector)
- t : sampling time
- $p(s)$: ideal RSS (dBm)
- $d(s)$: distance from AP to MD (m)
- (p_0, d_0) : reference RSS p_0 sampled at distance from an AP (dBm, m)
- $n(s)$: path loss induced by NLOS errors and wall-penetration factors
- $m(t)$: temporal RSS variation
- α : signal attenuation factor
- $v(s,t)$: white Gaussian measurement noise

In Eq. (1), p_0 , d_0 , and α with respect to an AP can be determined by sampling RSS measurements at various MD locations where the line-of-sight signal path between the MD and the AP is guaranteed. The spatially-correlated path loss $n(s)$ includes the NLOS errors [18] and wall-penetration factors caused by complex indoor geometric environments. The temporal RSS variation $m(t)$ includes

channel congestion and contention related with an AP. The measurement noise $v(s,t)$ is assumed to be wide-sense stationary (WSS) white Gaussian in both space and time domains.

The ESPM shown in Eq. (1) considers both spatial and temporal errors at the same time. If the time index t and the signal variation $m(t)$ in Eq. (1) are eliminated, it is reduced to the conventional SPM [15-18].

2.2 State space model of temporal variation

The temporal variation $m(t)$ of the proposed ESPM can be modeled, in its simplest but effective form, as the WSS first-order Markov process satisfying the following equation.

$$m(t + \Delta t) = \exp \left[-\frac{|\Delta t|}{\tau_t} \right] m(t) + \int_t^{t+\Delta t} w(\tau) d\tau \quad (2)$$

where τ_t is the correlation time and $w(t)$ is the white Gaussian noise in temporal domain. The autocorrelation of $w(t)$ can be expressed as

$$E[w(t)w(t+\tau)] = q_w \delta(\tau) \quad (3)$$

The notation $E[\cdot]$ shown in Eq. (3) denotes the statistical expectation. Due to the whiteness of the noise $w(t)$, the autocorrelation of $m(t)$ is

$$E[m(t)m(t+\tau)] = c_m \exp \left[-\frac{|\tau|}{\tau_t} \right] \quad (4)$$

From Eqs. (2)-(4), the analytic variogram $\gamma(\tau)$ of RSS measurements can be modeled by

$$\begin{aligned} \gamma(\tau) &= \frac{1}{2} E[\tilde{p}(s,t+\tau) - \tilde{p}(s,t)]^2 \\ &= c_m \left[1 - \exp \left(-\frac{|\tau|}{\tau_t} \right) \right] + c_v \end{aligned} \quad (5)$$

As shown in Eq. (5), the variogram depends on c_m , c_v , and τ_t . To extract these parameters, an experimental variogram [19] can be pre-computed based on the real measurement as.

$$\tilde{\gamma}(\tau) = \frac{1}{2M} \sum_{k=1}^M [\tilde{p}(s,t_k) - \tilde{p}(s,t_k + \tau)]^2 \quad (6)$$

where M denotes the number of measurement pairs utilized in deriving the experimental variogram. By comparing the analytic variogram and the experimental

variogram, the unknown parameters c_m , c_v , and τ_t can be obtained.

2.3 State space model of spatial variation

A state space model to describe RSS variations in spatial domain is required to derive an efficient spatial interpolation algorithm. For the purpose, the RSS measurement $\tilde{p}(s, t)$ shown in Eq. (1) is decomposed into the mean $\mu(t)$, the spatial variation $\delta\mu(s)$, and the white-Gaussian measurement noise $v(s, t)$

$$\tilde{p}(s, t) = \mu(t) + \delta\mu(s) + v(s, t) \quad (7)$$

where $\mu(t)$ is the unknown spatial mean at t over the entire deployment area A of the location system. The spatial mean $\mu(t)$ and the WSS spatial variation $\delta\mu(s)$ are modeled to satisfy the following equations.

$$\mu(t) = m(t) + \frac{1}{A} \int_A \tilde{p}(s, t) ds \quad (8)$$

$$\delta\mu(s + \Delta s) = \exp\left[-\frac{\|\Delta s\|}{\tau_s}\right] \delta\mu(s) + \int_s^{s+\Delta s} \eta(l) dl \quad (9)$$

where τ_s is the correlation distance and $\eta(s)$ is the white Gaussian noise in spatial domain. The autocorrelation of $\eta(s)$ is

$$E[\eta(s)\eta(s+l)] = q_\eta \delta(\|l\|) \quad (10)$$

Hence the autocorrelation of $\delta\mu(s)$ can be represented as

$$E[\delta\mu(s)\delta\mu(s+l)] = c_\mu \exp\left[-\frac{\|l\|}{\tau_s}\right] \quad (11)$$

It is modeled that the spatial white noise $\eta(s)$ is independent of the temporal white noise $w(t)$ for any s and t . As a result, $\delta\mu(s)$ is independent of $m(t)$ (refer to Eqs. (2) and (9)).

$$E[\delta\mu(s)m(t)] = 0 \quad (12)$$

Hence the spatial and temporal variations can be treated independently.

The analytic variogram $\gamma(l)$ of RSS measurement in spatial domain can be modeled as

$$\begin{aligned} \gamma(l) &= \frac{1}{2} E[\tilde{p}(s+l, t) - \tilde{p}(s, t)]^2 \\ &= c_\mu \left[1 - \exp\left(-\frac{\|l\|}{\tau_s}\right) \right] + c_v \end{aligned} \quad (13)$$

The analytic variogram depends on c_μ , c_v , and τ_s . Similarly to Eq. (6), the following experimental variogram can be pre-computed

$$\tilde{\gamma}(l) = \frac{1}{2N} \sum_{k=1}^N [\tilde{p}(s_k + l, t) - \tilde{p}(s_k, t)]^2 \quad (14)$$

where N denotes the number of measurement pairs utilized in deriving the experimental variogram. By comparing the analytic variogram and the experimental variogram, the unknown parameters c_μ , c_v , and τ_s can be obtained.

3. Spatiotemporal Fingerprint Generation

3.1 Overall algorithm structure

In the proposed location fingerprint generation method, two types of locations need to be discriminated; sampling locations (SLs) and reference locations (RLs). An SL corresponds to the location where RSS measurements are actually sampled. An RL corresponds to the location where a location fingerprint is generated.

The overview of the proposed method for spatiotemporal fingerprint generation is shown in Fig. 1. RSS measurements are sampled at several SLs and the Kalman filters are applied to these measurements for each SL. Then the Kriging estimator combines the outputs of Kalman filters to generate the reference fingerprints associated with dense RLs which are regular grid points.

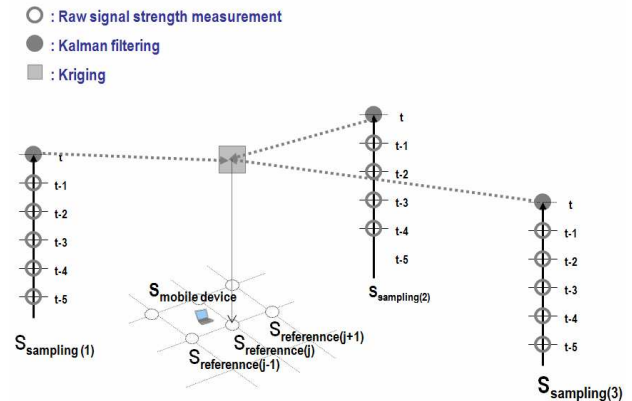


Fig. 1. Overview of the processing structure to generate spatiotemporal location fingerprints

Recursive Kalman filtering is advantageous in reducing the computational burden to process sampled measurements. Kriging is beneficial in generating location fingerprints at arbitrary many RLs based on few sampled measurements. The two attractive estimators are connected by the ESPM which is discussed in detail in this section.

3.2 Temporal filtering

From now on, a Kalman filter algorithm based on the ESPM is formulated for temporal filtering. The states of Kalman filter are selected as

$$X(s_k, t_i) = \begin{bmatrix} p(s_k) + n(s_k) \\ m(t_i) \end{bmatrix} \quad (15)$$

where s_k denotes an SL which is fixed and known and t_i is a discrete sampling time instant. Hence the system model for time propagations and measurement updates can be obtained as follows based on Eqs. (1)-(15).

$$X(s_k, t_{i+1}) = FX(s_k, t_i) + G\omega(t_i) \quad (16)$$

$$\tilde{p}(s_k, t_i) = HX(s_k, t_i) + v(s_k, t_i) \quad (17)$$

where

$$\begin{aligned} F &= \begin{bmatrix} 1 & 0 \\ 0 & \exp(-T_s / \tau_t) \end{bmatrix}, \quad G = \begin{bmatrix} 0 \\ 1 \end{bmatrix}, \quad H = [1 \quad 1] \\ T_s &= t_{i+1} - t_i \quad (\text{fixed sampling interval}) \\ \omega(t_i) &= \int_{t_i}^{t_i+T_s} w(\tau) d\tau \sim N(0, c_\omega) \\ c_\omega &= [1 - \exp(-2T_s / \tau_t)] c_m \\ v(s_k, t_i) &\sim N(0, c_v) \end{aligned} \quad (18)$$

The notation $X \sim N(\bar{X}, C_X)$ denotes that the random vector X satisfies the Gaussian distribution with the mean vector \bar{X} and the covariance matrix C_X .

Based on the modeling by Eqs. (16)-(18), the initialization, the time propagation, and the measurement update stages of each Kalman filter are formulated as follows

Initialization:

$$\begin{aligned} \hat{X}(s_k, t_0) &= \begin{bmatrix} \tilde{p}(s_k, t_0) \\ 0 \end{bmatrix} \\ C(s_k, t_0) &= \begin{bmatrix} 1 & 1 \\ 0 & -1 \end{bmatrix} \begin{bmatrix} c_v & 0 \\ 0 & c_m \end{bmatrix} \begin{bmatrix} 1 & 0 \\ 1 & -1 \end{bmatrix} \end{aligned} \quad (19)$$

Time Propagation:

$$\begin{aligned} \bar{X}(s_k, t_{i+1}) &= F\hat{X}(s_k, t_i) \\ \bar{C}(s_k, t_{i+1}) &= FC(s_k, t_i)F^T + Gc_\omega G^T \end{aligned} \quad (20)$$

Measurement Update :

$$\begin{aligned} K(s_k, t_i) &= \bar{C}(s_k, t_i)H^T \left(H\bar{C}(s_k, t_i)H^T + c_v \right)^{-1} \\ \hat{X}(s_k, t_i) &= \bar{X}(s_k, t_i) + K(s_k, t_i) \left[\tilde{p}(s_k, t_i) - H\bar{X}(s_k, t_i) \right] \\ C(s_k, t_i) &= [I - K(s_k, t_i)H] \bar{C}(s_k, t_i) [I - K(s_k, t_i)H]^T \\ &\quad + K(s_k, t_i)c_v [K(s_k, t_i)]^T \end{aligned} \quad (21)$$

The output of the Kalman filter satisfies the following equation.

$$\begin{aligned} H\hat{X}(s_k, t_i) &= H \left[X(s_k, t_i) + \delta\hat{X}(s_k, t_i) \right] \\ &= p(s_k) + n(s_k) + m(t_i) + H\delta\hat{X}(s_k, t_i) \end{aligned} \quad (22)$$

where

$$\begin{aligned} \delta\hat{X}(s_k, t_i) &\triangleq \hat{X}(s_k, t_i) - X(s_k, t_i) \quad : \text{estimation error} \\ \delta\hat{X}(s_k, t_i) &\sim (0, C(s_k, t_i)) \end{aligned} \quad (23)$$

It should be noted that $H\delta\hat{X}(s_k, t_i)$ in Eq. (22) plays the similar role as that of $v(s, t)$ in Eq. (1) of a single RSS measurement. However, the variance of $H\delta\hat{X}(s_k, t_i)$ is smaller than that of the single measurement noise $v(s, t)$ after several measurement updates of the Kalman filter since the pair (F, H) is completely observable.

$$HC(s_k, t_i)H^T < c_v \quad (24)$$

3.3 Spatial filtering

While the Kalman filters are running at several SLs, the spatiotemporal location can be generated by applying the Kriging algorithm to the Kalman filter outputs at each time step. In the proposed method, the location fingerprints can be generated for arbitrarily many RLs utilizing the reference RSS measurements sampled at few SLs. To apply the Kriging algorithm, the output of each Kalman filter is interpreted differently as follows.

$$\begin{aligned} H\hat{X}(s_k, t_i) &= p(s_k) + n(s_k) + m(t_i) + H\delta\hat{X}(s_k, t_i) \\ &= \mu(t_i) + \delta\mu(s_k) + H\delta\hat{X}(s_k, t_i) \end{aligned} \quad (25)$$

In general, the estimation error $\delta\hat{X}(s_k, t_i)$ of the Kalman filter is the combination of the initial estimation error $\delta\hat{X}(s_k, t_0)$, the propagation noises $\{\omega(t_j)\}$, and the measurement noises $\{v(s_k, t_j)\}$ up to the current instant. Since $\delta\hat{X}(s_k, t_0)$, $\{\omega(t_j)\}$, and $\{v(s_k, t_j)\}$ are independent of the spatial variation $\delta\mu(s_k)$, it holds that

$$E\left[\delta\mu(s_k)\delta\hat{X}(s_k,t_i)\right]=0 \quad (26)$$

for any t_i .

Once the reference RSS values are prepared at the several SLs by the Kalman filters, the location fingerprints at any RL can be generated. For the purpose, the proposed method utilizes Kriging algorithm since it is based on the well-developed statistical theory for spatial analysis [19], robust to modeling errors [20], and closely connected with Kalman filtering.

Before applying Kriging algorithm at the i -th time step, a measurement vector is obtained by accumulating K scalar measurements as follows.

$$Z(t_i) = L\mu(t_i) + \mathcal{E}(t_i) \quad (27)$$

where

$$Z(t_i) = \begin{bmatrix} z(s_1,t_i) \\ z(s_2,t_i) \\ \vdots \\ z(s_K,t_i) \end{bmatrix} = \begin{bmatrix} H\hat{X}(s_1,t_i) \\ H\hat{X}(s_2,t_i) \\ \vdots \\ H\hat{X}(s_K,t_i) \end{bmatrix}, \quad L = \begin{bmatrix} 1 \\ \vdots \\ 1 \end{bmatrix},$$

$$\mathcal{E}(t_i) = \begin{bmatrix} \varepsilon(s_1,t_i) \\ \varepsilon(s_2,t_i) \\ \vdots \\ \varepsilon(s_K,t_i) \end{bmatrix} = \begin{bmatrix} \delta\mu(s_1) + H\delta\hat{X}(s_1,t_i) \\ \delta\mu(s_2) + H\delta\hat{X}(s_2,t_i) \\ \vdots \\ \delta\mu(s_K) + H\delta\hat{X}(s_K,t_i) \end{bmatrix}.$$

K : number of SLs (28)

Based on Eq. (27) the best linear unbiased estimate $\hat{Z}_j(s_0,t_i)$ of the location fingerprint at an arbitrary RL $s_0 = [x_0 \ y_0]^T$ can be obtained by applying the following Kriging algorithm [19, 20].

$$\hat{\mu}(t_i) = (L^T \Gamma_{\varepsilon\varepsilon}^{-1} L)^{-1} L^T \Gamma_{\varepsilon\varepsilon}^{-1} Z(t_i)$$

$$\hat{Z}(s_0,t_i) = \hat{\mu}(t_i) + \Gamma_{0\varepsilon}^T \Gamma_{\varepsilon\varepsilon}^{-1} [Z(t_i) - L\hat{\mu}(t_i)] \quad (29)$$

where

$$\Gamma_{\varepsilon\varepsilon} = \begin{bmatrix} \gamma_{11} & \gamma_{12} & \cdots & \gamma_{1K} \\ \gamma_{21} & \gamma_{22} & \cdots & \gamma_{2K} \\ \vdots & \vdots & \ddots & \vdots \\ \gamma_{K1} & \gamma_{K2} & \cdots & \gamma_{KK} \end{bmatrix}$$

$$\Gamma_{0\varepsilon} = [\gamma_{01} \ \gamma_{02} \ \cdots \ \gamma_{0K}]^T$$

$$\gamma_{kl} = c_\mu \left[1 - \exp\left(-\frac{\|s_k - s_l\|}{\tau_s}\right) \right]$$

$$+ \frac{1}{2} H [C(s_k,t_i) + C(s_l,t_i)] H^T$$

$$\gamma_{0k} = c_\mu \left[1 - \exp\left(-\frac{\|s_0 - s_k\|}{\tau_s}\right) \right] + \frac{1}{2} H C(s_k,t_i) H^T \quad (30)$$

In Eq. (30), γ_{kl} denotes the variogram between the SLs where measurements are actually sampled and γ_{0k} denotes the variogram between an RL and an SL. It should be noted again that RLs do not require actual measurement sampling.

As shown above, three parameters c_μ , τ_s , and $C(s_k,t_i)$ affect the evaluation of the variograms. The two parameters c_μ and τ_s can be obtained by comparing the empirical and analytic variograms (refer to Eqs. (13) and (14)). The covariance $C(s_k,t_i)$ can be calculated from the Kalman filter corresponding to the k -th SL and the i -th sampling time.

4. Experiment

4.1 Temporal variations of received signal strength

To characterize temporal variations of WLAN RSS measurements, an experiment was performed. For the purpose, RSS measurements were collected with respect to a public AP which belongs to a network which provides wireless connections to the students in a university building. The RSS measurements were collected during six successive days by utilizing a laptop computer at fixed location. According to the conventional SPM, the RSS measurements sampled at a fixed location are expected to be constant since the geometry between the MD and the AP does not change. In Fig. 2, the raw and smoothed RSS trends are depicted as thin and thick lines, respectively. The smoothed RSS trend was obtained by averaging successive fifty RSS measurements. Each thin vertical line appearing at regular interval corresponds to the noon of each day.

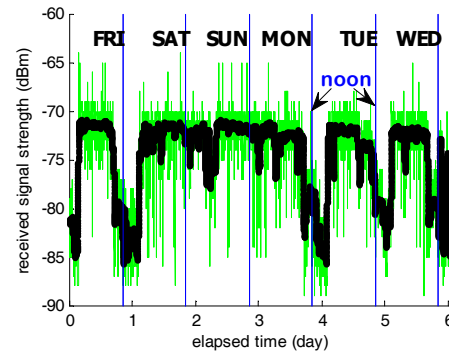


Fig. 2. Trends of received signal strength measurements; raw (thin gray line) and smoothed (thick black line)

In Fig. 2, an interesting characteristic can be found in the smoothed RSS trend. The RSS level becomes low during

working hours in weekdays such as Friday, Monday, Tuesday, and Wednesday. During night hours, the RSS level is mostly high. On the other hand, the RSS magnitude does not drop down largely on Saturday and Sunday. Thus, the long-term RSS trend bears a significant component of one day period obeying two types of patterns; weekday and weekend. Since large decrease in RSS level occurs only during working hours on weekdays, it seems that the RSS temporal variation is closely related to the number of people within the AP's signal range.

The large RSS variation that appears during weekdays can be attributed to two factors; the movements of people within the signal path from the AP to the laptop computer and the channel conditions occurred by many WLAN users in the form of congestion, contention, and interference. Among the two main factors, the effects of the movements of people cannot persist more than several minutes if we consider walking speed of people and the AP's signal range. Thus, it is strongly estimated that the large variations that appears during weekdays are caused by the channel conditions due to the increase number of WLAN users.

4.2 Performance of spatiotemporal fingerprint

To evaluate the performance of the proposed method, an experiment was performed. The layout of the test bed is indicated in Fig. 3 which corresponds to a floor in a university building that consists of offices, lecture rooms, and laboratories. It should be noted that most of people move along the corridors within 10 minute period during each hour since the test bed corresponds to a university building.

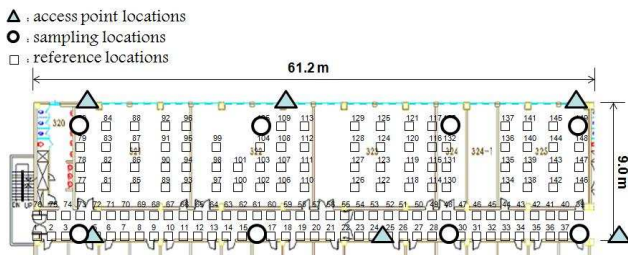


Fig. 3. Experimental test bed.

A laptop computer was utilized to collect the RSS measurements at various RLs. There are in total 6 APs, 8 SLs and 140 RLs. The spacing between two adjacent SLs is about 9 to 20 meters. Obviously, the number of SL is much smaller than that of RLs. Measurements were collected in six periods during two successive weekdays which are summarized in Table 1. An illustrative distribution of average RSS values is depicted in Fig. 4.

To obtain the key parameters such as c_μ , c_v , τ_s , c_m , c_v , and τ_t , experimental variograms were extracted by applying the collected measurements to Eqs. (6) and (14). The key parameters were selected as follows so that

Table 1. Six different periods to collect signal strength measurements for location fingerprints generation

Notation	Time Interval
PERIOD 1	13:00-15:00 PM
PERIOD 2	17:00-19:00 PM
PERIOD 3	21:00-23:00 PM
PERIOD 4	01:00-03:00 AM
PERIOD 5	05:00-07:00 AM
PERIOD 6	09:00-11:00 AM

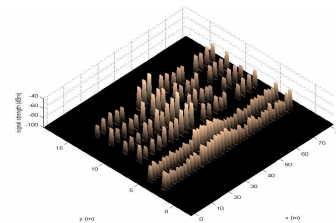


Fig. 4. An example distribution of average signal strength measurements over the experiment area

the analytic variogram based on Eqs. (5) and (13) are consistent with the experimental variograms.

$$c_\mu = 100 \text{ (dBm}^2\text{)}, c_v = 5 \text{ (dBm}^2\text{)}, \tau_s = 10 \text{ (m)} \quad (31)$$

$$c_m = 1.8 \text{ (dBm}^2\text{)}, c_v = 5 \text{ (dBm}^2\text{)}, \tau_t = 3600 \text{ (sec)} \quad (32)$$

The key parameters were utilized to generate seven sets of location fingerprints: six sets of spatial fingerprints which correspond to six testing periods (i.e. the data collected in each period were used to generate a set of spatial fingerprints) by applying the spatial Kriging algorithm based on the conventional SPM without considering the temporal characteristics. In addition, one set of spatiotemporal fingerprint was generated by applying the proposed method.

To test the different sets of fingerprints, a set of testing data were collected during PERIOD 6 at various test locations. For each test location, RSS measurements were sampled for 5 seconds to obtain an average value. The true values of the test locations' position were obtained by utilizing grid lines marked on the floor.

It should be noted that there is no common location between the SLs and the test locations. However, the RLs are the same as the test locations in this experiment.

To obtain MD position estimates, the simplest nearest neighbor algorithm was utilized to test the effectiveness of the proposed method. The average RSSs collected at each test locations were compared with the fingerprint vectors in the database. The RL corresponding to the best matched fingerprint vector was determined as the location of the user.

The positioning accuracy when different fingerprint database were used is shown in Fig. 5. As the testing data were collected at PERIOD 6, there are time differences between this period and the periods when differences between this period and the periods when reference data

were collected at SLs (i.e. PERIOD1 to PERIOD6).

In Fig. 5, it can be seen that the time difference is an important factor. The positioning accuracy deteriorates significantly when the time difference is 12 and 16 hours.

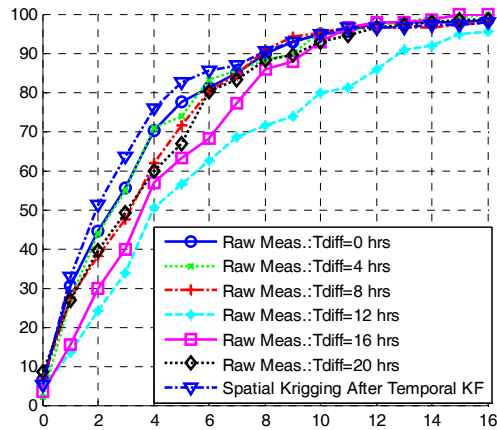


Fig. 5. Comparison of cumulative probabilities of error distances by applying spatial location fingerprints and spatiotemporal location fingerprint

However, the accuracy is much better when the time difference is 0, 4, 8, and 20 hours. This result is consistent with the previous experiment result showing that the long-term RSS variation bears a significant component corresponding to the period of 24 hours. Thus, signal difference becomes largest if time difference is near 12 hours.

Fig. 4 also reveals that when the spatiotemporal fingerprint is utilized, the best accuracy can be achieved. Since the test data were collected at PERIOD 6, it is fair to compare the positioning result using the fingerprint database generated by applying the spatial Kriging algorithm to the data collected in PERIOD 6 with that of the proposed method. The circular error probable (CEP) values are about 2.5 m and 1.9 m respectively which means the improvement of accuracy is about 24% due to the utilization of more measurements in a correct way.

5. Conclusion

This paper proposes an extended signal propagation model and a spatiotemporal location fingerprint generation method to improve the positioning accuracy using fingerprinting technology based on received signal strength measurements. First, the extended signal propagation model which can cope with both the spatial and temporal variations of signal strength measurements in one framework is proposed. Then an efficient spatiotemporal location fingerprint generation method based on Kalman filtering and Kriging algorithm is formulated. To verify the efficiency of the proposed method, an experiment was carried out. The results show that the positioning accuracy

can be improved by at least 24% if temporal variations are considered in addition to the spatial dependence of the receive signal strength measurements.

Acknowledgements

This research was supported by Basic Science Research Program (2010-0010899) through the National Research Foundation of Korea(NRF) funded by the Ministry of Education, Science and Technology, Korea.

References

- [1] Y. Chen and H. Kobayashi, "Signal strength based indoor geolocation," *IEEE International Conference on Communications*, pp. 436-439, 2002.
- [2] Y. Wang, X. Jia, H. K. Lee, and G. Y. Li, "An indoor wireless positioning system based on wireless local area network," *International Symposium on Satellite Navigation Technology Including Mobile Positioning and Location Services*, paper 54, 2003.
- [3] Y. Qi, *Wireless Geolocation in a Non-Line-of-Sight Environment*, Ph.D. dissertation, Princeton University, November 2003.
- [4] A. Bahillo, S. Mazuelas, R. M. Lorenzo, P. Fernandez, J. Prieto, R. J. Duran, and E. J. Abril, "Hybrid RSS-RTT Localization Scheme for Indoor Wireless Networks," *EURASIP Journal on Advances in Signal Processing*, Article ID 126082, 2010.
- [5] P. Bahl, V. N. Padmanabhan, and A. Balachandran, *A software system for locating mobile users: Design, evaluation, and lessons*, Technical report, Microsoft Research, 2000.
- [6] P. Bahl and V. N. Padmanabhan, "RADAR: An in-building RF-based user location and tracking system," *IEEE INFOCOM*, pp. 775-784, 2000.
- [7] J. Krumm and J.C. Platt, *Minimizing Calibration Effort for an In-door 802.11 Device Location Measurement System*, Technical Report, Microsoft Research, 2003.
- [8] B. Li, Y. Wang, H.K. Lee, A. Dempster and C. Rizos, "Method for yielding a database of location fingerprints in WLAN," *IEE Proceedings-Communications*, vol. 152, no. 5, pp. 580-586, 2005.
- [9] X. Chai and Q. Yang, "Reducing the Calibration Effort for Location Estimation Using Unlabeled Samples," *IEEE PerCom*, 2005.
- [10] M. Youssef and A. Agrawala, "Small-scale compensation for WLAN location determination systems," *IEEE WCNC*, pp. 1974-1978, 2003.
- [11] S. Ganu, A. S. Krishnakumar, and P. Krishnan, "Infrastructure-based location estimation in WLAN networks," *IEEE WCNC*, pp. 465-470, 2004.

- [12] H. Akima, "A new method of Interpolation and Smooth Curve Fitting based on Local Procedures," *Journal of the ACM*, vol. 17, no. 4, pp. 589-602, 1970.
- [13] Y. Gwon and R. Jain, "Error characteristics and calibration-free techniques for wireless LAN-based location estimation," *ACM MobiWac*, 2004.
- [14] K. Kaemarungsi, *Design of indoor positioning systems based on location fingerprinting technique*, Ph.D. dissertation, University of Pittsburgh, 2005.
- [15] S. Pandey, B. Kim, F. Anjum, and P. Agrawal, "Client assisted location data acquisition scheme for secure enterprise wireless network," *IEEE WCNC*, pp. 1174-1179, 2005.
- [16] H. Lim, L. C. Kung, J. C. Hou, and H. Luo, "Zero-configuration, robust indoor localization: theory and experimentation," *IEEE INFOCOM*, pp. 1-12, 2006.
- [17] A. Kushki, K. N. Plataniotis, and A. N. Venetsanopoulos, "Kernel-Based Positioning in Wireless Local Area Networks," *IEEE Tr: Mobile Computing*, Vol. 6, No. 6, pp. 689-705, 2007
- [18] H. K. Lee, J. Y. Shim, H. S. Kim, B. Li, and C. Rizos, "Feature Extraction and Spatial Interpolation for Improved Wireless Location Sensing", *Sensors*, Vol. 8, pp. 2865-2885, 2008
- [19] N. A. C. Cressie, *Statistics for spatial data*. John Wiley & Sons, 1993.
- [20] J. Lefebvre, H. Roussel, E. Walter, D. Lecointe, and W. Tabbara, "Prediction from wrong models: the Kriging approach," *IEEE Antennas and Propagation Magazine*, vol. 38, no. 4, pp. 35-45, 1996.



Hee Sung Kim He received the B.S. and M.S. degrees in the School of Electronics, Telecomm., and Computer Engineering at Korea Aerospace University, Korea, in 2007 and 2009, respectively. He is a doctoral course student at Navigation and Information Systems Lab., Korea Aerospace University. His research interests include positioning systems, satellite navigation systems, GPS/GNSS network, and estimation theory.



Binghao Li He is a VC's Post-Doctoral Research Fellow at the School of Surveying and Spatial Information Systems, The University of New South Wales, Sydney, Australia. He obtained B.Sc. in Electrical & Mechanical Eng. from Northern Jiaotong University, P.R. China in 1994 and M.Sc. in Civil Eng., Tsinghua University, P.R. China in 2001. He received his Ph.D. from the University of New South Wales, Sydney, Australia in 2006. His research area is pedestrian navigation, new positioning technologies.



Wan Sik Choi He received the BS degree in the Department of Mechanical Engineering from Sung Kyun Kwan University, Korea in 1979, the MS degrees in the Mechanical Engineering and the Applied Mathematics from The Univ. of Alabama, U.S.A in 1986, 1988 respectively. He received the Ph.D. degree in the Department of Mechanical Engineering from The Univ. of Alabama in 1992. He was with the ADD from 1979 to 1984 as a researcher. Since 1992, he has been with ETRI as a Senior/Principal Member of Research Staff. His research interests include positioning, LBS, satellite system and optimal control.



Sang Kyung Sung He received the B.S. and Ph.D. degrees in Electrical Engineering from Seoul National University, Korea, in 1996 and 2003, respectively. From March 1996 to February 2003, he worked for the Automatic Control Research Center in Seoul National University. Currently, he is an Associate Professor of the Department of Aerospace Information Engineering, Konkuk University. His research interests include avionic system and IT fusion technology, inertial sensors, integrated navigation, and application to unmanned systems.



Hyung Keun Lee He received the B.S. and M.S. degrees in control and instrumentation engineering and the Ph.D. degree from the School of Electrical Engineering and Computer Science from Seoul National University, Korea, in 1990, 1994, and 2002, respectively. From 1994 to 2002, he was with Hyundai Aerospace Co. Ltd as a researcher. From Sept. 2002 to Aug. 2003, he was with the School of Surveying and Spatial Information Systems, UNSW, Sydney, Australia as a post-doctoral research fellow. Since 2003, he has been with the School of Electronics, Telecomm., and Computer Engineering at Korea Aerospace Univ., Korea, as an associate professor. His research interests include positioning, navigation, and transportation systems.